Environmental Science & Technology

Article

pubs.acs.org/est

Molecular Selectivity of Brown Carbon Chromophores

Julia Laskin,*[,†] Alexander Laskin,*[,‡] Sergey A. Nizkorodov,[§] Patrick Roach,[†] Peter Eckert,[‡] Mary K. Gilles,[∥] Bingbing Wang,[‡] Hyun Ji (Julie) Lee,[§] and Qichi Hu[†]

[†]Physical Sciences Division and [‡]Environmental Molecular Sciences Laboratory, Pacific Northwest National Laboratory, Richland, Washington 99352, United States

[§]Department of Chemistry, University of California, Irvine, California 92697, United States

[∥]Chemical Sciences Division, Lawrence Berkeley National Laboratory, Berkeley, California 94720, United States

Supporting Information

ABSTRACT: Complementary methods of high-resolution mass spectrometry and microspectroscopy were utilized for molecular analysis of secondary organic aerosol (SOA) generated from ozonolysis of two structural monoterpene isomers: D-limonene SOA (LSOA) and α-pinene SOA (PSOA). The LSOA compounds readily formed adducts with Na^+ under electrospray ionization conditions, with only a small fraction of compounds detected in the protonated form. In contrast, a significant fraction of PSOA compounds appeared in the protonated form because of their increased molecular rigidity. Laboratory simulated aging of LSOA and PSOA, through conversion of carbonyls into imines mediated by NH_3 vapors in humid air, resulted in selective browning of the LSOA sample, while the PSOA sample remained white. Comparative analysis of the reaction products in the aged LSOA and PSOA samples provided insights into chemistry relevant to formation of brown carbon chromophores. A significant fraction of carbonyl-imine conversion products with identical molecular formulas was detected in both samples. This reflects the high level of similarity in the molecular composition of these two closely related SOA materials. Several highly conjugated products were detected exclusively in the brown LSOA sample and were identified as potential chromophores responsible for the observed color change. The majority of the unique products in the aged LSOA sample with the highest number of double bonds contain two nitrogen atoms. We conclude that chromophores characteristic of the carbonyl-imine chemistry in LSOA are highly conjugated oligomers of secondary imines (Schiff bases) present at relatively low concentrations. Formation of this type of conjugated compounds in PSOA is hindered by the structural rigidity of the α-pinene oxidation products. Our results suggest that the overall light-absorbing properties of SOA may be determined by trace amounts of strong brown carbon chromophores.

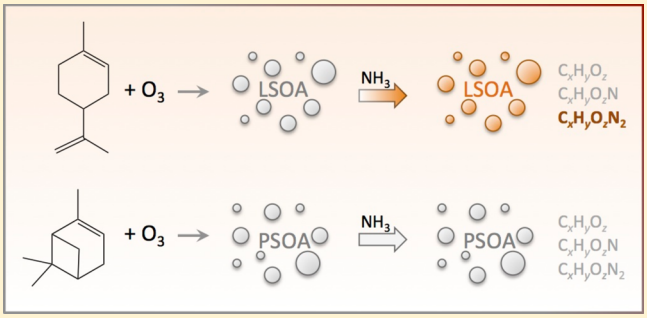

INTRODUCTION

Light-absorbing organic aerosol (i.e., brown carbon, BrC) has recently been recognized as a significant climate forcing factor.[1,2] However, limited knowledge of the chemical composition and physical properties of BrC hinders understanding of the mechanisms and rates of its formation and transformation in the atmosphere. Biomass burning has been identified[2,3] as a major source of BrC. Substituted aromatics formed in biomass-burning and residential coal combustion were reported[3,4] as light-absorbing chromophores in ambient aerosol. In addition, various high molecular weight (high-MW) compounds (in excess of ~300 Da) produced in atmospheric multiphase reactions between gas-phase, particulate, and cloud microdroplet constituents may also contribute to light absorption. Examples include NO_3-mediated oxidation of various volatile organic compounds (VOCs; especially polycyclic aromatic hydrocarbons, PAHs) leading to formation of nitro and nitrooxy compounds in secondary organic aerosol (SOA);[5,6] reactions of OH radicals with aromatic hydroxy acids in cloud water;[7] heterogeneous reactions of gaseous isoprene on acidic aerosol particles;[8] aqueous reactions of glyoxal in the presence of ammonium sulfate or amino acids;[9−13] and NH_3-mediated carbonyl-to-imine reactions of secondary organic aerosols.[14−16]

Recent studies demonstrated that reduced nitrogen species (such as ammonia, organic amines, and amino acids) efficiently react with atmospherically prevalent carbonyl compounds to form BrC products.[9−22] For example, chemical aging of biogenic SOA formed by ozonolysis of D-limonene (LSOA) in the presence of ammonia results in efficient browning of SOA material, which has been attributed to carbonyl-to-imine conversion.[14−16,18] We hypothesized[21] that the chromophores responsible for the observed browning of LSOA are highly conjugated species containing molecular moieties of secondary imines (Schiff bases). It has also been demonstrated that formation of BrC chromophores depends on the initial structure

Received: July 16, 2014
Revised: September 14, 2014
Accepted: September 18, 2014
Published: September 18, 2014

of the carbonyl species involved in the process. For example, while the vast majority of the SOA constituents are susceptible to the carbonyl-to-imine conversion, only a small subset of these species lead to BrC formation.[21] Due to the inherent complexity of SOA, identification of specific BrC chromophores is challenging. In this study, we address this challenge by comparing the molecular composition of LSOA and α-pinene SOA (PSOA), two closely related SOA systems, after identical exposures to gaseous ammonia and humid air. Identical aging processes result in efficient browning for LSOA and no change in the PSOA color. Because limonene and α-pinene are structural isomers, this comparison provides information on the effect of the organic precursor chemical structure on the chemical aging and the light-absorbing properties of SOA.

EXPERIMENTAL SECTION

Generation and Aging of SOA Samples. LSOA and PSOA samples were generated through ozone-initiated oxidation of D-limonene (>98% purity, Sigma-Aldrich, Inc.) and α-pinene (>98% purity, Sigma-Aldrich, Inc.), respectively, as described elsewhere.[23,24] Briefly, SOA samples were produced in an inflatable ~400 L Teflon reaction chamber by injecting 10 μL of a mixture containing 25 vol % of the precursor terpene and 75 vol % cyclohexane (HPLC grade) in the presence of 2 ppm of ozone generated by a commercial generator (Pacific Ozone, Model L11/R-LAB111) and measured by a UV photometric O_3 analyzer (Thermo Electron, Inc.). The resulting SOA was collected after ~90 min onto Teflon (polytetrafluoroethylene, PTFE) 46.2 mm ring supported membranes (GE Healthcare Bio-Sciences, Inc.) using a ten stage rotating Micro-Orifice Uniform Deposition Impactor (MOUDI, model 110R, MSP Corporation). The collected particles were deposited fairly uniformly over a 27 mm diameter impaction area. Silicon wafer chips (10 × 10 mm^2) and Si_3N_4 thin film windows (Silson Ltd.) were mounted on the PTFE membranes to collect particle samples for analysis using infrared reflection absorption spectroscopy (IRRAS) and transmission X-ray spectro-microscopy techniques. Most of the SOA samples described in this manuscript were collected on the eighth stage of MOUDI, which corresponds to particles in a size range of 0.18−0.32 μm aerodynamic diameter. The eighth stage was chosen to facilitate comparison with our previous studies.[15,23,25−29] Larger particles in a size range of 0.56−1.0 μm (the sixth stage of the impactor) were collected for the X-ray spectro-microscopy analysis of individual particles.

Chemical aging of SOA samples was performed as described elsewhere.[15,16] Specifically, the Teflon membrane with the collected SOA was attached to a plastic plate and allowed to float in a covered Petri dish on the surface of a 0.1 M aqueous solution of NH_4NO_3 (Sigma-Aldrich Inc., 99.99% purity). It is estimated[15] that SOA samples were exposed to equilibrium partial pressures of $NH_{3(g)}$ ($<1.2 \times 10^{-7}$ atm) and $HNO_{3(g)}$ ($<1.6 \times 10^{-13}$ atm) and RH in excess of 85% for 24 h.

Infrared Reflection Absorption Spectroscopy (IRRAS). Grazing-incidence IRRAS experiments[30,31] utilized a Bruker Vertex 70 Fourier transform infrared (FTIR) spectrometer (Bruker, Billerica, MA) equipped with a liquid nitrogen cooled mercury−cadmium−telluride (MCT) detector. IRRAS spectra were obtained at a resolution of 4 cm^{-1} using p-polarized light. The angle of incidence was 80° with respect to the surface normal. Each spectrum was collected from a film of SOA material deposited on silicon wafer chips and acquired for 2 min corresponding to an average of 512 scans. The IR beam path was purged with the nitrogen gas. A blank silicon wafer chip was used as a background.

Scanning Transmission X-ray Microscopy (STXM). Carbon bonding in fresh versus aged individual LSOA particles deposited over the Si_3N_4 filmed substrate was probed using the STXM instrument at beamline 11.0.2 of the Advanced Light Source at Lawrence Berkeley National Laboratory. In these experiments, the intensity of a narrowly focused X-ray beam transmitted through a particle sample was measured at fixed energies within the carbon K-edge absorption (280−320 eV). The sample was raster scanned at each of the energies to record a "stack" of images from which near edge X-ray absorption fine structure (NEXAFS) spectra of individual particles were extracted. Additional details of particle analysis using STXM/NEXAFS can be found elsewhere.[32−34]

High Resolution Mass Spectrometry (HR-MS). Fresh and aged LSOA and PSOA samples were analyzed using a high resolution LTQ-Orbitrap mass spectrometer (Thermo Electron, Bremen, Germany) equipped with a custom built nanospray desorption electrospray ionization source (nano-DESI).[35,36] The heated inlet capillary of the instrument was maintained at 250 °C. The mass spectrometer was operated in the positive ion mode with a resolving power of $\sim 10^5$ at m/z 400. The instrument was calibrated daily using a standard mixture of caffeine, MRFA, and Ultramark 1621 (calibration mix MSCAL 5, Sigma-Aldrich, Inc.). Analysis of the LSOA and PSOA samples deposited on the PTFE membranes was performed by bringing the sample in contact with the nano-DESI probe.

Following the procedures described in our previous publications,[28,29,35] the background signal was acquired in each experiment by placing the probe on the part of the PTFE substrate that was free of SOA for 1−2 min during data acquisition. The probe was subsequently moved to the SOA covered area of the sample, and the signal was acquired for another 3−4 min. Background peaks could be distinguished from the analyte peaks by their time dependence during the data acquisition. Specifically, background peaks typically show a significant decrease when the nano-DESI probe is placed on the sample due to the presence of other analyte molecules competing for ionization.[35] Mass spectra were subsequently obtained by averaging the signal over the time window during which the nano-DESI probe was in contact with the SOA sample.

HR-MS data were analyzed as described in our previous studies.[37,38] Specifically, peaks with a signal-to-noise ratio of 5 and higher were extracted from the spectra using Decon2LS (http://ncrr.pnl.gov/software/). The background peaks were removed by aligning the spectrum of the sample with the corresponding background spectrum and eliminating most of the features observed in the background spectrum except for the peaks occurring with a minimum of 2.5 times greater intensity in the spectrum of the sample than in the background. Peaks corresponding to ions containing ^{13}C isotopes were eliminated as well. The signal peaks were subsequently grouped using the first- and second-order mass defect analysis described elsewhere.[38] Formula assignments were performed using the MIDAS Molecular Formula Calculator (http://www.magnet.fsu.edu/usershub/scientificdivisions/icr/icr_software.html).

RESULTS AND DISCUSSION

The chemical mechanisms of NH_3-mediated aging of SOA are complex, but the initial steps involve reactions illustrated by Schemes R1 and R2. Following its uptake into SOA particles, ammonia reacts with carbonyls forming primary

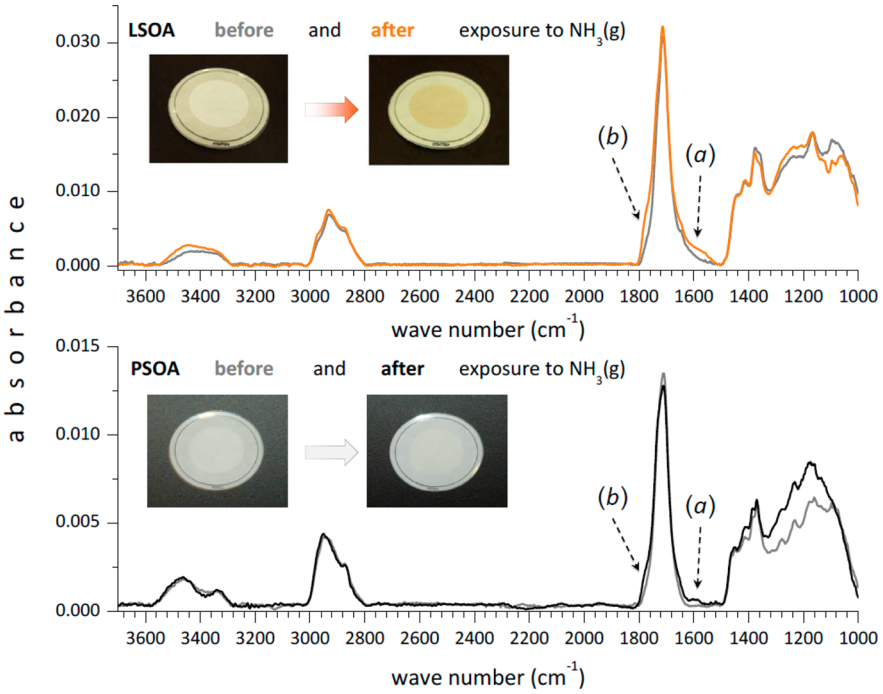

Figure 1. Photographs and IRRAS spectra of LSOA and PSOA samples before and after exposure to NH_3. Dashed arrows draw attention to the relatively weak absorption bands next to the strong carbonyl peak (1700 cm^{-1}) indicative of the carbonyl-imine chemistry. The bands are attributable to (a) Schiff base (secondary imines) products (~1600 cm^{-1}) and (b) secondary oxidation products of Schiff bases (~1750 cm^{-1}).

imines and amines. These transient products continue to react with unreacted carbonyls forming condensation (oligomer) products containing more stable secondary imines (Schiff bases) (reaction Scheme R1).

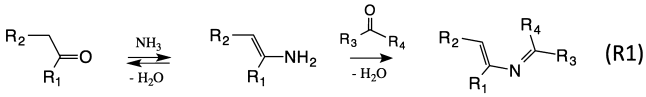

Some of the SOA compounds possess multiple carbonyl groups allowing intramolecular cyclization into products with N-heterocyclic structures. For instance, reaction Scheme R2 illustrates plausible N-heterocyclic cyclization of keto-limonone-aldehyde (KLA), a major product of D-limonene ozonolysis, resulting in formation of a pyrrole derivative. KLA is selected as an example because of its critical importance to BrC formation in LSOA.[21] However, many other LSOA components and their derivatives may undergo intramolecular cyclization forming N-heterocycles of different sizes (pyridines, pyrazines, imidazoles, etc.).

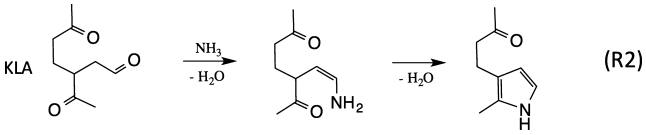

Products of reaction sequences R1 and R2 continue to react forming larger oligomers through intermolecular carbonyl-imine and aldol condensation reactions. In the case of LSOA, these reaction sequences result in formation of oligomeric products with extensive conjugation of π-bonds creating the BrC chromophores that contribute to the overall orange-to-brown color of the reacted sample. In contrast, PSOA does not display the browning effect which indicates that the molecular structures of its constituents are critically important in the formation of BrC through reactions with ammonia.

Figure 1 shows photographs of LSOA and PSOA samples before and after laboratory aging experiments with NH_3, along with their corresponding IRRAS spectra. Visual appearance of the aged LSOA and PSOA samples is remarkably different indicating browning of LSOA and no color change of PSOA in agreement with our previous reports.[16] Changes in the mass absorption coefficients (MAC) upon NH_3-mediated aging were quantified on the basis of UV–vis measurements with the reported wavelength-averaged $<\Delta MAC_{300-700\ nm}>$ values of 400 and 50 $cm^2\ g^{-1}$ for LSOA and PSOA, respectively.[16] The details of these measurements and the definition of $<\Delta MAC_{300-700\ nm}>$ are included in Figure S1 of the Supporting Information file. Although UV–vis absorption properties of the LSOA and PSOA aged spectra are different, their IRRAS spectra are very similar. Comparison of the IRRAS spectra acquired from the same samples before and after NH_3-aging experiments show only minor changes in their overall chemical composition. Carbonyl-to-imine conversions are indicated by a minor buildup of two bands at ~1600 cm^{-1} (band a) and ~1750 cm^{-1} (band b) adjacent to the shoulders of the strong carbonyl peak (1700 cm^{-1}). Bands a and b can be attributed to the formation of N-heteroatom products through reaction R1. Specifically, band a is consistent with the C=N stretching mode reported[39] in a range of 1616–1643 cm^{-1} for different secondary imines (Schiff bases); band b is consistent with the red-shifted C=O stretching mode reported[40] in a range of 1720–1780 cm^{-1} for compounds with mixed carboxyl-imine moieties such as alanines and oxazolidinones.

Minor changes in the overall composition of the LSOA sample resulting from NH_3-mediated aging were corroborated by the X-ray absorption spectroscopy of individual SOA particles (see Figure S2 of the Supporting Information file for details). Combined together, IRRAS and NEXAFS data indicate that NH_3-mediated reactions do not appreciably change the overall composition of the SOA materials but rather induce formation of

small quantities of N-containing products. Assuming the same absorption cross sections for carbonyl (~1700 cm^{-1}) and Schiff base (~1600 cm^{-1}) groups contributing to the broad (1500–1800 cm^{-1}) IRRAS feature, we estimate that the overall extent of the carbonyl-to-imine conversion is less than 5% for both LSOA and PSOA samples. Furthermore, only a small fraction of these products may have light-absorbing properties relevant to BrC chromophores, and the BrC chromophores are selectively formed only in the LSOA material.

We used the nano-DESI/HR-MS platform to probe molecule-specific differences in the fresh and aged samples of LSOA and PSOA. Positive mode mass spectra of SOA typically contain both protonated $[M + H]^+$ and sodiated $[M + Na]^+$ molecules. The source of sodium available for ionization is usually related to minor impurities leached from the analytical glassware and may vary significantly between the samples. In this study, a controlled amount of NaCl was added to the working solvent to maximize the extent of sodium adduct formation in the analysis of LSOA and PSOA samples. Figure 2 shows HR-MS data obtained for fresh LSOA and

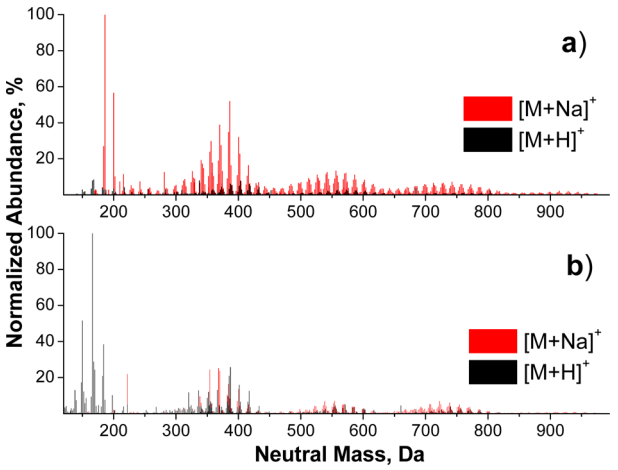

Figure 2. Assigned peaks in nano-DESI high resolution mass spectra of (a) fresh LSOA and (b) fresh PSOA. Normalized abundances of the peaks are plotted against the corresponding neutral masses to facilitate comparison. Protonated molecules are shown in black; sodiated species are shown in red.

PSOA samples using 20 μM NaCl in acetonitrile as a solvent to facilitate the formation of $[M + Na]^+$ ions. Systematic examination of the effect of the NaCl concentration on the observed peak distribution showed that at this concentration of NaCl the sodium adduct formation for compounds in LSOA reaches saturation (data not shown). Both LSOA and PSOA spectra contain characteristic peaks corresponding to monomeric oxidation products (typically with 9 or 10 carbon atoms) along with dimers, trimers, and tetramers. However, while a majority of peaks in the LSOA spectrum correspond to $[M + Na]^+$ ions, ozonolysis products of α-pinene were observed as both $[M + Na]^+$ and $[M + H]^+$ species. To facilitate the comparison between LSOA and PSOA spectra, Figure 2 displays neutral masses of all the peaks assigned in the spectra (more than 90% of the detected peaks were assigned). In both spectra, black traces correspond to species observed as $[M + Na]^+$ adducts, while molecules observed as $[M + H]^+$ species are highlighted in red. Although distributions of neutral masses obtained for LSOA and PSOA samples are similar,

Table 1. Number of Protonated and Sodiated Peaks in the HR-MS Spectra Corresponding to Oxygenated Organic Compounds without Nitrogen Atoms (CHO) in Nano-DESI/HR-MS Spectra of Fresh LSOA and PSOA Samples

	LSOA	PSOA
assigned CHO peaks	837	778
number of $[CHO + Na]^+$ ions	826	633
number of $[CHO + H]^+$ ions	39	270
peaks observed as both $[CHO + Na]^+$ and $[CHO + H]^+$	28	125

the modes of ionization of the components in the two mixtures are strikingly different. Table 1 is a summary of the number of assigned peaks in both spectra corresponding to oxygenated $C_xH_yO_z$ compounds that do not contain nitrogen atoms (CHO). The number of peaks corresponding to $[M + H]^+$ species increases from 5% for LSOA to 35% for PSOA. Most of the $[M + H]^+$ peaks in the LSOA spectrum are also observed as sodiated species. In contrast, the extent of overlap between the populations of $[M + H]^+$ and $[M + Na]^+$ ions in the PSOA spectrum is significantly smaller meaning that a majority of molecules are observed as either $[M + H]^+$ or $[M + Na]^+$ ions.

Normalized abundances of the peaks corresponding to $[M + H]^+$ and $[M + Na]^+$ ions of the primary ozonolysis products of D-limonene and α-pinene are summarized in Table S1, Supporting Information. Most of the primary ozonolysis products reported in previous studies[23,24] are observed in nano-DESI spectra. Surprisingly, limonaldehyde and keto-limonaldehyde, observed by Walser et al.[24] as major peaks in ESI-MS, are only minor features in the nano-DESI spectrum of the fresh LSOA sample examined in this study. Because of the high reactivity of the aldehyde group, these primary products may undergo secondary reactions on filters prior to analysis. Most of the observed primary ozonolysis products of α-pinene are protonated species. Interestingly, two structural isomers, pinonic and limononic acids, are observed as $[M + H]^+$ and $[M + Na]^+$ ions, respectively, of approximately equal intensity.

The difference in the mode of ionization of compounds in LSOA and PSOA is related to structural differences between the isomeric species present in these mixtures. Specifically, the embedded cyclobutane ring contained in the primary products of α-pinene ozonolysis (e.g., pinonaldehyde (PA), norpinonic acid, 10-hydroxylpinonaldehyde, norpinonaldehyde, and pinonic and pinic acids) result in rigid structures that cannot readily solvate sodium cations. In contrast, the products of limonene ozonolysis (e.g., limonic acid, limononic acid, KLA, and other products in which the limonene endocyclic C=C bond is severed by ozone) have more flexible structures that have better affinity to sodium cations (see, for example, the structures of KLA and PA shown below).

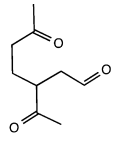

Keto-Limonone-Aldehyde (KLA)

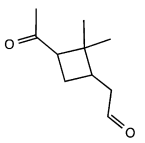

Pinone-Aldehyde (PA)

It is reasonable to assume that the ozonolysis products of limonene have more flexible structures with higher sodium affinities, which facilitates the formation of $[M + Na]^+$ species. Although gas-phase basicities of terpenes and their ozonolysis products are not known, the relative trends can be inferred from the known ionization energies (IE). Correlations of the gas-phase

basicity with core IE have been reported for many classes of compounds,[41] for which ionization occurs on the same site as protonation. Molecules with higher electron binding energy (corresponding to higher IE) have lower propensity to share electron density with the ionizing proton. As a result, the gas-phase basicity decreases with increasing IE. Because the IE of limonene (8.07 eV) is lower than the IE of α-pinene (8.3 eV), it is reasonable to assume that the gas-phase basicity of α-pinene is higher than that of limonene. Facile protonation of the PSOA constituents indicate that this trend in the gas-phase basicity is largely preserved for all PSOA products. Interestingly, while protonation is the major ionization mode for monomeric species in the PSOA spectrum, a significant fraction of dimers and all trimers and tetramers are observed as $[M + Na]^+$ ions. This observation provides further support that sodium adduct formation in the PSOA analysis is affected by the flexibility of the molecule that increases from monomers to dimers to larger oligomers. Facile formation of $[M + Na]^+$ ions in the analysis of LSOA and PSOA is consistent with previous studies.[15,22,24]

Figure 3 and Table 2 show the effect of NH_3-mediated chemical aging on the types of species detected in the samples.

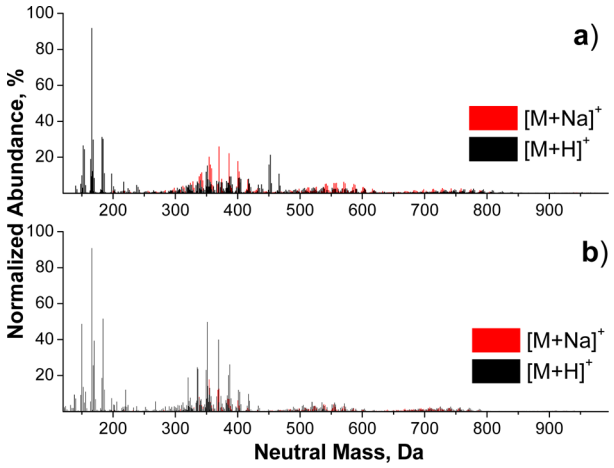

Figure 3. Assigned peaks in nano-DESI high resolution mass spectra of (a) NH_3-aged LSOA and (b) NH_3-aged PSOA. Normalized abundances of the peaks are plotted against the corresponding neutral masses to facilitate comparison. Protonated molecules are shown in black; sodiated species are shown in red.

Table 2. Number of CHO, CHON1, and CHON2 Species Detected (as Either Protonated or Sodiated Molecules) in the Fresh and Aged LSOA and PSOA Samples

compound type	LSOA	PSOA	common species in both LSOA and PSOA	unique for LSOA	unique for PSOA
			Fresh Samples		
CHO	837	778	464	373	314
CHON1	234	360	135	99	225
CHON2	0	0	0	0	0
			Aged Samples		
CHO	647	670	414	233	256
CHON1	701	611	430	271	181
CHON2	188	3	0	188	3

The results indicate that chemical aging of LSOA and PSOA results in formation of compounds containing one and two nitrogen atoms (CHON1 and CHON2). We note that spectra of the fresh SOA samples already contain a number of CHON1 species. In our previous study,[15,27] we showed that these peaks correspond to poorly controlled background reactions of SOA constituents with trace amounts of ammonia in laboratory air. However, the number of CHON1 peaks shows a significant increase (from 234 to 701 in LSOA and from 360 to 611 in PSOA) following exposure to NH_3. In addition, new peaks corresponding to oxygenated organic compounds (CHO) are also observed in the spectra of aged LSOA and PSOA. These compounds are most likely produced through hydrolysis of the primary SOA products.

Figure 4 shows a more detailed comparison between the mass spectra of aged LSOA and PSOA with separate color

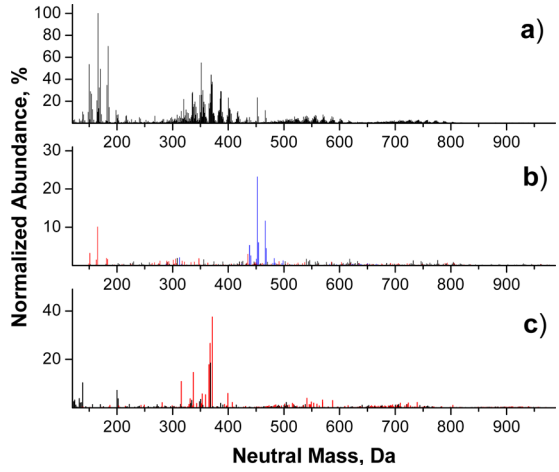

Figure 4. Panel (a): assigned peaks observed in both aged LSOA and aged PSOA samples (combined data sets). Panel (b): peaks unique for aged LSOA. Panel (c): peaks unique for aged PSOA. Normalized abundances of the peaks are plotted against the corresponding neutral masses to facilitate comparison. Normalized abundances of molecules observed both as protonated and sodiated species were added up. In panels (b) and (c), mass spectral features containing no nitrogen atoms (CHO) are shown in black, and species containing one and two nitrogen atoms (CHON1 and CHON2) are shown in red and blue, respectively.

coding of the CHO, CHON1, and CHON2 compounds. The number of overlapping and unique peaks in LSOA and PSOA is shown in Table 2. The most abundant peaks corresponding to CHO, CHON1, and CHON2 compounds in all four samples are listed in Table S2, Supporting Information. It is important to note that there is a significant overlap between the spectra of aged LSOA and PSOA samples. Specifically, 64% of CHO and CHON1 compounds are observed in *both* LSOA and PSOA spectra (Figure 4a and Table S2, Supporting Information). This degree of similarity is reasonable because the samples are produced by ozonolysis of structural isomers, limonene and α-pinene. Figure 4b,c shows neutral compounds unique to the aged LSOA and aged PSOA samples, respectively. Detailed comparison of the data shown in Figure 4 and listed in Table S2, Supporting Information, indicates that chemical aging has only a minor effect on the distribution of the CHO compounds. One notable exception is the $C_{10}H_{14}O_2$ (166.0994 Da) species, which is a relatively small feature in the spectrum of fresh LSOA but is the most abundant peak in the other three spectra (aged LSOA, fresh PSOA, aged PSOA). The relative abundance of this peak is strongly dependent on the amount of sodium cations in the system. Specifically, at low sodium concentrations, the ion

dx.doi.org/10.1021/es503432r | Environ. Sci. Technol. 2014, 48, 12047−12055

at m/z 167.1067 corresponding to $[C_{10}H_{14}O_2 + H]^+$ is the most abundant feature in the spectrum of the fresh LSOA sample, while at higher sodium concentrations, $[C_9H_{14}O_4 + Na]^+$ at m/z 209.0784 and $[C_{10}H_{16}O_4 + Na]^+$ at m/z 223.0941 dominate the spectrum.

Several abundant CHON1 species including $C_{20}H_{35}NO_5$, $C_{20}H_{35}NO_6$, $C_{20}H_{35}NO_7$, $C_{19}H_{33}NO_6$, and $C_{19}H_{33}NO_7$ are observed in the fresh PSOA sample. In contrast with several other CHON1 molecules, the relative abundances of these species do not change significantly after chemical aging with ammonia. This indicates that they are produced from very reactive precursors that are rapidly consumed either during SOA formation or briefly after the aerosol is collected on the substrate and exposed to air prior to analysis. Relative abundances of several CHON1 molecules, for example, $C_9H_{11}NO_2$, $C_9H_{13}NO_2$, $C_{19}H_{29}NO_4$, $C_{19}H_{29}NO_5$, and $C_{19}H_{33}NO_5$ are significantly enhanced in the aged LSOA and PSOA samples. Interestingly, the majority of abundant CHON1 species are observed in both aged LSOA and PSOA samples. In contrast, the CHON2 species are observed almost exclusively in the aged LSOA sample (Table S2, Supporting Information). CHON2 species account for more than 12% of all the observed features in the spectrum of aged LSOA (188 peaks). In contrast, only 3 low-abundance CHON2 compounds are observed in the spectrum of aged PSOA. The unique CHON2 molecules in the aged LSOA sample include products with elemental formulas characteristic of trimers and tetramers formed through the reaction sequence R1 and R2, e.g., $C_{27}H_{36}N_2O_4$, $C_{28}H_{38}N_2O_4$, and $C_{28}H_{38}N_2O_5$ trimers; $C_{37}H_{46}N_2O_4$, $C_{37}H_{50}N_2O_8$, and $C_{37}H_{52}N_2O_7$ tetramers. Molecules containing more than 2 nitrogen atoms are not readily observed in either aged PSOA or aged LSOA samples.

Figure 5 shows a plot of double bond equivalent (DBE) values, the total number of double bonds and rings calculated on the basis of assigned formulas, of various species found in aged LSOA and PSOA samples, plotted as a function of the number of carbon atoms in their structures.[37] The data are shown along with the reference DBE values characteristic of the highest possible number of conjugated double bonds in linear polyenes with a general formula C_xH_{x+2} (dashed line) and the highest possible number of double bonds and cycles in *cata*-condensed PAHs (solid line).[42] Compared to all other species in the spectrum of the aged LSOA, the CHON2 species have the highest DBE values, indicating they are the most conjugated of the detected products and therefore may be responsible for the absorption of the UV/visible light by the aged LSOA. We note that a conversion of a carbonyl to imine in the first step of R1 does not change DBE; however, subsequent intramolecular (R1) or intermolecular (R2) condensation reactions lead to an increase in DBE. More than one water molecule must be lost to afford the high observed DBE values. For example, trimer and tetramer CHON2 species detected in the aged LSOA samples may potentially have up to 12 and 15 conjugated bonds, respectively. This level of conjugation would be sufficient[43,44] for absorption of visible light, especially if the location of the nitrogen atoms in the molecule favors charge transfer transitions as, for example, in the classic case of cyanine dyes. Comparison of their DBE values with respect to the C_xH_{x+2} reference values indicates that the conjugation of π-bonds in these species is localized over most, but not all, of their carbon skeleton. If they contain cyclic structures, the overall length of the conjugated system could be even shorter.

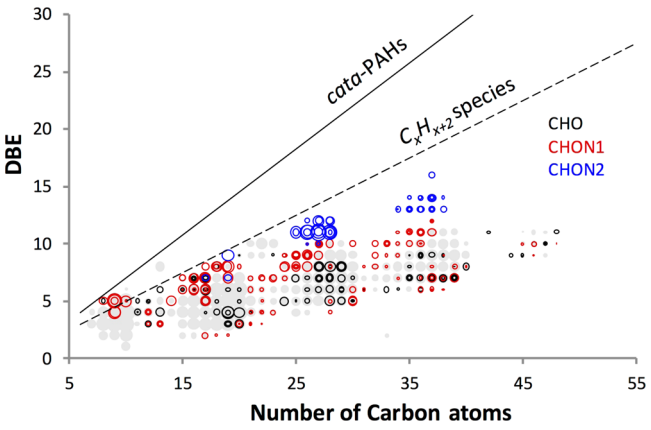

Figure 5. DBE vs number of carbon atoms plots obtained from assigned MS features in aged LSOA and PSOA samples. Gray solid symbols indicate common features detected in both samples. Open symbols highlight CHO (black), CHON1 (red), and CHON2 (blue) species unique to LSOA samples. Symbol size is proportional to the logarithmic intensity of corresponding peaks. Lines indicate reference DBE values of *cata*-condensed PAHs (solid line) and C_xH_{x+2} species (dashed line). High-molecular weight species of CHON2 composition in the closest proximity to the C_xH_{x+2} limit are plausible BrC chromophores.

Efficient absorption of visible light requires uninterrupted conjugation across a significant part of the molecular skeleton. This requirement is harder to fulfill in products of PSOA + NH_3 reactions compared to the LSOA + NH_3 products. All products with the highest DBE values detected in the aged PSOA sample are substantially less conjugated, because each of the monomer units of PSOA preserves a four membered ring. For example, according to the data shown in Figure 5, the highest DBE values corresponding to the trimer and the tetramer species in PSOA are 10 and 11, respectively. Since DBE values include the number of rings in the molecules and each monomer unit in PSOA contains one ring, the highest number of conjugated π-bonds in the aged trimers and tetramers of PSOA is only 7. Even if all 7 π-bonds are conjugated, its length would be too short for the absorption of visible light and longer wavelengths.[43,44] Similarly, because of the significant overlap between the CHON1 compounds observed in the spectra of aged LSOA and PSOA and the relatively low DBE values obtained for these species, it is unlikely that the CHON1 products of the chemical aging of LSOA and PSOA contribute to the observed changes in the light absorbing properties of the SOA material. On the basis of the results of this study, we conclude that, although the PSOA material undergoes extensive chemical aging as a result of the carbonyl-imine reactions, its products do not contain BrC chromophores, which require unique and molecular-specific precursors. In contrast to PSOA, the inherent flexibility of the LSOA molecular precursors facilitates the formation of BrC chromophores through carbonyl-imine chemistry and multistep condensation reactions.

This study clearly shows that visible light absorption by organic aerosols is exquisitely sensitive to molecular composition. Table 3 shows averaged values of O/C, H/C, and N/C atomic ratios characteristic for the SOA samples examined in this study. The calculation assumes that ESI efficiencies are equal between the SOA constituents, and the reported ratios are calculated using the abundance weighted atomic ratios in individual molecules. Utility of this approach has been established in our previous works for quantitative description of SOA mixtures and tracking their evolution in various aging processes.[45−48] The nearly identical averaged atomic ratios

Table 3. Median Number of C Atoms and Average Ratios of H/C, O/C, and N/C Characteristic for LSOA and PSOA Samples before and after NH_3-Mediated Aging[a]

	median number of C atoms in detected species	<H/C>	<O/C>	<N/C>
fresh LSOA	28	1.58	0.39	<0.01
aged LSOA	26	1.57	0.34	0.02
fresh PSOA	28	1.58	0.32	0.01
aged PSOA	27	1.59	0.31	0.02

[a]The ratios are calculated on the basis of the abundance weighted atomic ratios in individual molecules.[45]

characteristic of the LSOA and PSOA samples before and after NH_3-mediated aging suggests that formation of BrC materials cannot be predicted using bulk measurements. Although the BrC chromophores are clearly minority compounds, which do not significantly contribute to the average molecular composition of SOA, they exert a disproportionate level of influence on the SOA absorption coefficient. It follows that detailed characterization of the molecular composition of BrC aerosols is necessary for understanding the effect of aerosol chemistry on the optical and chemical properties of this important class of complex atmospheric particles.

Formation of BrC chromophores in LSOA is not limited to the gas-particle uptake of NH_3; similar browning reactions of LSOA and resilience to browning of PSOA were also reported for their aqueous mixtures with ammonium sulfate.[16,18,21] Therefore, some of the aging processes discussed in this work should also be relevant to reactions of monoterpene SOA compounds in cloud droplets, fog droplets, and deliquesced ammonium sulfate aerosols. Because of the widespread distribution of monoterpene and ammonia emissions, these browning reactions may have global significance. The reported MAC values of ~500 $cm^2\ g^{-1}$ (an average over the visible spectrum) characteristic of brown LSOA suggest that its global effects on the radiative forcing would be relatively minor, but not negligible, compared to biomass burning aerosols for which MAC values at the level of 10^3–10^4 $cm^2\ g^{-1}$ were reported.[49] We should stress that the lack of browning in PSOA does not imply lack of reactivity toward NH_3; according to our measurements, the overall PSOA molecular composition changes as much as LSOA composition does upon exposure to NH_3. The assessment of the molecular selectivity of BrC chromophores presented in this work may have additional significance extending beyond the laboratory generated LSOA and PSOA systems studied here. However, detection of BrC compounds formed by the NH_3 aging chemistry in field samples remains challenging because it requires wavelength-resolved UV–vis absorption spectra, which are still limited for ambient aerosols. It is noteworthy that recent field measurements at several locations near Atlanta, GA, reported UV–vis spectra of biomass burning BrC material that contained a distinctive absorption band around 500 nm,[50] potentially suggesting the presence of similar chromophores in the field samples. It remains to be seen whether these types of BrC compounds are common in the environment; the molecular signatures of the chromophoric compounds discussed in this work should aid in their future identification in field samples.

■ ASSOCIATED CONTENT

Supporting Information

UV-vis spectra; STXM images; carbon-edge NEXAFS spectra; tables of normalized abundances of $[M + H]^+$ and $[M + Na]^+$ peaks corresponding to the major ozonolysis products of limonene and α-pinene in nano-DESI/HRMS spectra of fresh LSOA and PSOA samples and neutral masses (Da), normalized abundances (%), double bond equivalents (DBE), and formula assignments of the most abundant species identified in nano-DESI/HRMS spectra of the fresh and aged LSOA and PSOA. This material is available free of charge via the Internet at http://pubs.acs.org.

■ AUTHOR INFORMATION

Corresponding Authors

*E-mail: julia.laskin@pnnl.gov; phone: +1 509 376-6136; fax: +1 509 376-6139.

*E-mail: alexander.laskin@pnnl.gov; phone: +1 509 376-6129; fax: +1 509 376-6139.

Notes

The authors declare no competing financial interest.

■ ACKNOWLEDGMENTS

PNNL and UCI groups acknowledge support by the U.S. Department of Commerce, National Oceanic and Atmospheric Administration through Climate Program Office's AC4 program, awards NA13OAR4310066 (PNNL) and NA13OAR4310062 (UCI). The ESI-HR-MS and FTIR measurements were performed at the W.R. Wiley Environmental Molecular Sciences Laboratory (EMSL), a national scientific user facility located at PNNL, and sponsored by the Office of Biological and Environmental Research of the U.S. PNNL is operated for US DOE by Battelle Memorial Institute under Contract No. DE-AC06-76RL0 1830. J.L., Q.H., and P.R. acknowledge additional support from the DOE's Office of Basic Energy Sciences (BES), Division of Chemical Sciences, Geosciences & Biosciences. P.E. acknowledges support from the DOE Science Undergraduate Laboratory Internship program. STXM/NEXAFS measurements were done at Beamline 11.0.2 of the Advanced Light Source at Lawrence Berkeley National Laboratory (LBNL). The Advanced Light Source is supported by the Director, Office of Science, Office of Basic Energy Sciences, of the U.S. Department of Energy under Contract No. DE-AC02-05CH11231. M.K.G. and Beamline 11.0.2 are supported by the Director, Office of Science, Office of Basic Energy Sciences Division of Chemical Sciences, Geosciences, and Biosciences by the Condensed Phase and Interfacial Molecular Sciences Program of the U.S. Department of Energy at LBNL under Contract No. DE-AC02-05CH11231.

■ REFERENCES

(1) Bahadur, R.; Praveen, P. S.; Xu, Y.; Ramanathan, V. Solar absorption by elemental and brown carbon determined from spectral observations. *Proc. Natl. Acad. Sci. U.S.A.* **2012**, *109* (43), 17366–17371.

(2) Ramanathan, V.; Li, F.; Ramana, M. V.; Praveen, P. S.; Kim, D.; Corrigan, C. E.; Nguyen, H.; Stone, E. A.; Schauer, J. J.; Carmichael, G. R.; Adhikary, B.; Yoon, S. C. Atmospheric brown clouds: Hemispherical and regional variations in long-range transport, absorption, and radiative forcing. *J. Geophys. Res.: Atmos.* **2007**, *112*, (D22); DOI: 10.1029/2006jd008124.

(3) Andreae, M. O.; Gelencser, A. Black carbon or brown carbon? The nature of light-absorbing carbonaceous aerosols. *Atmos. Chem. Phys.* **2006**, *6*, 3131–3148.

(4) Bond, T.; Bergstrom, R. Light absorption by carbonaceous particles: An investigative review. *Aerosol Sci. Technol.* **2006**, *40* (1), 27–67.

(5) Jacobson, M. Z. Isolating nitrated and aromatic aerosols and nitrated aromatic gases as sources of ultraviolet light absorption. *J. Geophys. Res.: Atmos.* **1999**, *104* (D3), 3527−3542.
(6) Lu, J. W.; Flores, J. M.; Lavi, A.; Abo-Riziq, A.; Rudich, Y. Changes in the optical properties of benzo a pyrene-coated aerosols upon heterogeneous reactions with NO_2 and NO_3. *Phys. Chem. Chem. Phys.* **2011**, *13* (14), 6484−6492.
(7) Gelencser, A.; Hoffer, A.; Kiss, G.; Tombacz, E.; Kurdi, R.; Bencze, L. In-situ formation of light-absorbing organic matter in cloud water. *J. Atmos. Chem.* **2003**, *45* (1), 25−33.
(8) Limbeck, A.; Kulmala, M.; Puxbaum, H. Secondary organic aerosol formation in the atmosphere via heterogeneous reaction of gaseous isoprene on acidic particles. *Geophys. Res. Lett.* **2003**, *30* (19), 1996 DOI: 10.1029/2003GL017738.
(9) Galloway, M. M.; Chhabra, P. S.; Chan, A. W. H.; Surratt, J. D.; Flagan, R. C.; Seinfeld, J. H.; Keutsch, F. N. Glyoxal uptake on ammonium sulphate seed aerosol: Reaction products and reversibility of uptake under dark and irradiated conditions. *Atmos. Chem. Phys.* **2009**, *9* (10), 3331−3345.
(10) Noziere, B.; Dziedzic, P.; Cordova, A. Products and kinetics of the liquid-phase reaction of glyoxal catalyzed by ammonium ions (NH_4^+). *J. Phys. Chem. A* **2009**, *113* (1), 231−237.
(11) Shapiro, E. L.; Szprengiel, J.; Sareen, N.; Jen, C. N.; Giordano, M. R.; McNeill, V. F. Light-absorbing secondary organic material formed by glyoxal in aqueous aerosol mimics. *Atmos. Chem. Phys.* **2009**, *9* (7), 2289−2300.
(12) Trainic, M.; Riziq, A. A.; Lavi, A.; Flores, J. M.; Rudich, Y. The optical, physical and chemical properties of the products of glyoxal uptake on ammonium sulfate seed aerosols. *Atmos. Chem. Phys.* **2011**, *11* (18), 9697−9707.
(13) Kampf, C. J.; Jakob, R.; Hoffmann, T. Identification and characterization of aging products in the glyoxal/ammonium sulfate system - implications for light-absorbing material in atmospheric aerosols. *Atmos. Chem. Phys.* **2012**, *12* (14), 6323−6333.
(14) Bones, D. L.; Henricksen, D. K.; Mang, S. A.; Gonsior, M.; Bateman, A. P.; Nguyen, T. B.; Cooper, W. J.; Nizkorodov, S. A. Appearance of strong absorbers and fluorophores in limonene-O-3 secondary organic aerosol due to NH_4^+-mediated chemical aging over long time scales. *J. Geophys. Res.: Atmos.* **2010**, *115* (D5); DOI: 10.1029/2009JD012864.
(15) Laskin, J.; Laskin, A.; Roach, P. J.; Slysz, G. W.; Anderson, G. A.; Nizkorodov, S. A.; Bones, D. L.; Nguyen, L. Q. High-resolution desorption electrospray ionization mass spectrometry for chemical characterization of organic aerosols. *Anal. Chem.* **2010**, *82* (5), 2048−2058.
(16) Updyke, K. M.; Nguyen, T. B.; Nizkorodov, S. A. Formation of brown carbon via reactions of ammonia with secondary organic aerosols from biogenic and anthropogenic precursors. *Atmos. Environ.* **2012**, *63*, 22−31.
(17) De Haan, D. O.; Corrigan, A. L.; Tolbert, M. A.; Jimenez, J. L.; Wood, S. E.; Turley, J. J. Secondary organic aerosol formation by self-reactions of methylglyoxal and glyoxal in evaporating droplets. *Environ. Sci. Technol.* **2009**, *43* (21), 8184−8190.
(18) Nguyen, T. B.; Lee, P. B.; Updyke, K. M.; Bones, D. L.; Laskin, J.; Laskin, A.; Nizkorodov, S. A. Formation of nitrogen- and sulfur-containing light-absorbing compounds accelerated by evaporation of water from secondary organic aerosols. *J. Geophys. Res.: Atmos.* **2012**, *117* (D1); DOI: 10.1029/2011JD016944.
(19) Noziere, B.; Esteve, W. Light-absorbing aldol condensation products in acidic aerosols: Spectra, kinetics, and contribution to the absorption index. *Atmos. Environ.* **2007**, *41* (6), 1150−1163.
(20) Zarzana, K. J.; De Haan, D. O.; Freedman, M. A.; Hasenkopf, C. A.; Tolbert, M. A. Optical properties of the products of alpha-dicarbonyl and amine reactions in simulated cloud droplets. *Environ. Sci. Technol.* **2012**, *46* (9), 4845−4851.
(21) Nguyen, T. B.; Laskin, A.; Laskin, J.; Nizkorodov, S. A. Brown carbon formation from ketoaldehydes of biogenic monoterpenes. *Faraday Discuss.* **2013**, *165*, 473−494.
(22) Flores, J. M.; Washenfelder, R. A.; Adler, G.; Lee, H. J.; Segev, L.; Laskin, J.; Laskin, A.; Nizkorodov, S. A.; Brown, S. S.; Rudich, Y. Complex refractive indices in the near-ultraviolet spectral region of biogenic secondary organic aerosol aged with ammonia. *Phys. Chem. Chem. Phys.* **2014**, *16* (22), 10629−10642.
(23) Bateman, A. P.; Nizkorodov, S. A.; Laskin, J.; Laskin, A. Time-resolved molecular characterization of limonene/ozone aerosol using high-resolution electrospray ionization mass spectrometry. *Phys. Chem. Chem. Phys.* **2009**, *11* (36), 7931−7942.
(24) Walser, M. L.; Desyaterik, Y.; Laskin, J.; Laskin, A.; Nizkorodov, S. A. High-resolution mass spectrometric analysis of secondary organic aerosol produced by ozonation of limonene. *Phys. Chem. Chem. Phys.* **2008**, *10* (7), 1009−1022.
(25) Laskin, A.; Smith, J. S.; Laskin, J. Molecular characterization of nitrogen-containing organic compounds in biomass burning aerosols using high-resolution mass spectrometry. *Environ. Sci. Technol.* **2009**, *43* (10), 3764−3771.
(26) Smith, J. S.; Laskin, A.; Laskin, J. Molecular characterization of biomass burning aerosols using high-resolution mass spectrometry. *Anal. Chem.* **2009**, *81* (4), 1512−1521.
(27) Laskin, J.; Eckert, P. A.; Roach, P. J.; Heath, B. S.; Nizkorodov, S. A.; Laskin, A. Chemical analysis of complex organic mixtures using reactive nanospray desorption electrospray ionization mass spectrometry. *Anal. Chem.* **2012**, *84* (16), 7179−7187.
(28) O'Brien, R. E.; Laskin, A.; Laskin, J.; Liu, S.; Weber, R.; Russell, L. M.; Goldstein, A. H. Molecular characterization of organic aerosol using nanospray desorption/electrospray ionization mass spectrometry: CalNex 2010 field study. *Atmos. Environ.* **2013**, *68*, 265−272.
(29) O'Brien, R. E.; Nguyen, T. B.; Laskin, A.; Laskin, J.; Hayes, P. L.; Liu, S.; Jimenez, J. L.; Russell, L. M.; Nizkorodov, S. A.; Goldstein, A. H. Probing molecular associations of field-collected and laboratory-generated SOA with nano-DESI high-resolution mass spectrometry. *J. Geophys. Res.: Atmos.* **2013**, *118* (2), 1042−1051.
(30) Hadjar, O.; Wang, P.; Futrell, J. H.; Dessiaterik, Y.; Zhu, Z. H.; Cowin, J. P.; Iedema, M. J.; Laskin, J. Design and performance of an instrument for soft landing of biomolecular ions on surfaces. *Anal. Chem.* **2007**, *79* (17), 6566−6574.
(31) Hu, Q. C.; Wang, P.; Gassman, P. L.; Laskin, J. In situ studies of soft- and reactive landing of mass-selected ions using infrared reflection absorption spectroscopy. *Anal. Chem.* **2009**, *81* (17), 7302−7308.
(32) Moffet, R. C.; Henn, T. R.; Laskin, A.; Gilles, M. K. Automated chemical analysis of internally mixed aerosol particles using X-ray spectromicroscopy at the carbon K-edge. *Anal. Chem.* **2010**, *82* (19), 7906−7914.
(33) Moffet, R. C.; Henn, T. R.; Tivanski, A. V.; Hopkins, R. J.; Desyaterik, Y.; Kilcoyne, A. L. D.; Tyliszczak, T.; Fast, J.; Barnard, J.; Shutthanandan, V.; Cliff, S. S.; Perry, K. D.; Laskin, A.; Gilles, M. K. Microscopic characterization of carbonaceous aerosol particle aging in the outflow from Mexico City. *Atmos. Chem. Phys.* **2010**, *10* (3), 961−976.
(34) Moffet, R. C.; Tivanski, A. V.; Gilles, M. K. Scanning X-ray Transmission Microscopy: Applications in Atmospheric Aerosol Research. In *Fundamentals and Applications in Aerosol Spectroscopy*; Signorell, R., Reid, J. P., Eds.; CRC Press: Boca Raton, FL, 2010; pp 419−462.
(35) Roach, P. J.; Laskin, J.; Laskin, A. Molecular characterization of organic aerosols using nanospray-desorption/electrospray ionization-mass spectrometry. *Anal. Chem.* **2010**, *82* (19), 7979−7986.
(36) Roach, P. J.; Laskin, J.; Laskin, A. Nanospray desorption electrospray ionization: An ambient method for liquid-extraction surface sampling in mass spectrometry. *Analyst* **2010**, *135* (9), 2233−2236.
(37) Nizkorodov, S. A.; Laskin, J.; Laskin, A. Molecular chemistry of organic aerosols through the application of high resolution mass spectrometry. *Phys. Chem. Chem. Phys.* **2011**, *13* (9), 3612−3629.
(38) Roach, P. J.; Laskin, J.; Laskin, A. Higher-order mass defect analysis for mass spectra of complex organic mixtures. *Anal. Chem.* **2011**, *83* (12), 4924−4929.

(39) Lopezgarriga, J. J.; Babcock, G. T.; Harrison, J. F. Factors influencing the C═N stretching frequency in neutral and protonated schiff-bases. *J. Am. Chem. Soc.* **1986**, *108* (23), 7241−7251.
(40) Chu, F. L.; Yaylayan, V. A. FTIR monitoring of oxazolidin-5-one formation and decomposition in a glycolaldehyde-phenylalanine model system by isotope labeling techniques. *Carbohydr. Res.* **2009**, *344* (2), 229−236.
(41) Harrison, A. G. Special feature: Perspective - Linear free energy correlations in mass spectrometry. *J. Mass Spectrom.* **1999**, *34* (6), 577−589.
(42) Siegmann, K.; Sattler, K. Formation mechanism for polycyclic aromatic hydrocarbons in methane flames. *J. Chem. Phys.* **2000**, *112* (2), 698−709.
(43) Noziere, B.; Cordova, A. A kinetic and mechanistic study of the amino acid catalyzed aldol condensation of acetaldehyde in aqueous and salt solutions. *J. Phys. Chem. A* **2008**, *112* (13), 2827−2837.
(44) Noziere, B.; Dziedzic, P.; Cordova, A. Formation of secondary light-absorbing "fulvic-like" oligomers: A common process in aqueous and ionic atmospheric particles? *Geophys. Res. Lett.* **2007**, *34*, (21); DOI: 10.1029/2007gl031300.
(45) Bateman, A. P.; Laskin, J.; Laskin, A.; Nizkorodov, S. A. Applications of high-resolution electrospray ionization mass spectrometry to measurements of average oxygen to carbon ratios in secondary organic aerosols. *Environ. Sci. Technol.* **2012**, *46* (15), 8315−8324.
(46) Lee, H. J.; Aiona, P. K.; Laskin, A.; Laskin, J.; Nizkorodov, S. A. Effect of solar radiation on the optical properties and molecular composition of laboratory proxies of atmospheric brown carbon. *Environ. Sci. Technol.* **2014**, *48*, 10217−10226.
(47) Bateman, A. P.; Nizkorodov, S. A.; Laskin, J.; Laskin, A. Photolytic processing of secondary organic aerosols dissolved in cloud droplets. *Phys. Chem. Chem. Phys.* **2011**, *13* (26), 12199−12212.
(48) Nguyen, T. B.; Laskin, A.; Laskin, J.; Nizkorodov, S. A. Direct aqueous photochemistry of isoprene high-NOx secondary organic aerosol. *Phys. Chem. Chem. Phys.* **2012**, *14* (27), 9702−9714.
(49) Chen, Y.; Bond, T. C. Light absorption by organic carbon from wood combustion. *Atmos. Chem. Phys.* **2010**, *10* (4), 1773−1787.
(50) Liu, J.; Bergin, M.; Guo, H.; King, L.; Kotra, N.; Edgerton, E.; Weber, R. J. Size-resolved measurements of brown carbon in water and methanol extracts and estimates of their contribution to ambient fine-particle light absorption. *Atmos. Chem. Phys.* **2013**, *13* (24), 12389−12404.